U–Pb zircon dating of post-obduction volcanic-arc granitoids and a granulite-facies xenolith from New Caledonia. Inference on Southwest Pacific geodynamic models.

Jean-Louis Paquette, Dominique Cluzel

U-Pb ZIRCON DATING OF POST-OBDUCTION VOLCANIC-ARC GRANITOIDS AND A GRANULITE-FACIES XENOLITH FROM NEW CALEDONIA. INFERENCE ON SOUTHWEST PACIFIC GEODYNAMIC MODELS.

Jean-Louis Paquette[1*] and Dominique Cluzel[2]

[1] Laboratoire Magmas et Volcans UMR 6524, CNRS and Université B. Pascal, 5 rue Kessler, F-63038 Clermont-Ferrand cedex, France.

paquette@opgc.univ-bpclermont.fr

* corresponding author

[2] University of Orléans, Institut des Sciences de la Terre d'Orléans , UMR6113, BP 6759 F-45067 Orléans, France.

dominique.cluzel@univ-orleans.fr

Abstract.

In New Caledonia, the occurrence of one of the Wold's largest and best-exposed subduction/obduction complex is a key point for the understanding of the geodynamic evolution of the whole Southwest Pacific region. Within the ophiolite, pre-and post obduction granitoids intrude the ultramafic allochthon and provide new time constraints for the understanding of obduction processes. At 27.4 Ma, a new East-dipping subduction generated the active margin magmatism along the western coast of the island (Saint-Louis massif). At 24.3 Ma, the eastward shift of the magma activity and slightly different geochemical features (Koum-Borindi massif) was either related to the older slab break-off; or alternatively, due to the eastward migration of the mantle wedge following the collision of the eastern margin of the Low Howe rise. Finally, the occurrence of a granulite-facies xenolith in the Koum-Borindi massif with comparable 24.5 Ma U-Pb zircon age and isotopic features (initial ε_{Nd} = 5.1) suggests that these evolved magmas were generated within the lithospheric mantle beneath a continental crust of normal thickness. Geochronological evidence for continuous convergence during the Oligocene infers an East-dipping Eocene-Oligocene subduction/obduction system to have existed in the Southwest Pacific from the d'Entrecasteaux zone to the North Island of New Zealand.

Keywords: granitoid; granulite; U-Pb zircon geochronology; New Caledonia; active margin; Southwest Pacific.

Introduction.

The Southwest Pacific region consists of a complex set of submerged continental slices, volcanic arcs and marginal basins that mostly formed after the Early Cretaceous. Some of the geologic features exposed in this area may represent analogues of the pre-collision stage of many older orogenic belts. In New Caledonia, the Tertiary convergence resulted in one of the world's largest and best-exposed subduction/obduction complexes. It comprises upper Eocene blueschist-eclogite HP-LT terrane, foreland basins, peel off melange and ophiolite. The ophiolite of New Caledonia that bears nickel supergene ores of major economic importance is composed of a large harzburgite-dunite allochthon and minor mafic/ultramafic cumulates that represent the obducted fore-arc lithosphere of the Palaeocene-Eocene Loyalty arc. A variety of pre- and post-obduction felsic bodies (hereafter referred to as granitoids) intrude the ultramafic allochthon and are of some importance for the understanding of obduction process. This paper deals with the timing of post-obduction granitoids that intrude the ultramafic rocks and their basement. Here we present new age constraints on post-obduction magmatism based on ID-TIMS U-Pb zircon data. Whether or not the Tertiary subduction in New Caledonia continued after obduction and how long it did, is a major clue on Southwest Pacific evolution and allows regional correlations to be forwarded. These new data provide evidence for minor inheritance in some zircon cores; in addition, the occurrence of granulite-facies xenoliths that display the same U-Pb zircon age and similar isotopic signatures confirms that, contrary to a recent working hypothesis (Auzende et al. 2000), continental crust of normal thickness actually existed below the ultramafic allochthon soon after obduction.

Geologic setting.

Post-obduction granitoids of New Caledonia occur as kilometre-size plutons associated to a number of smaller dykes and stocks that are referred to as the St Louis and Koum-Borindi "granites". Both intrude the ophiolitic nappe and its basement, and develop narrow contact metamorphism aureoles. The ophiolite was obducted during the Late Eocene when the northern tip of the Norfolk-New Caledonia ridge, made of a detached slice of the Southeast-Gondwana margin, obliquely entered the East-dipping subduction zone of the Loyalty arc. Incipient subduction of buoyant crust material resulted in subduction blocking while slab roll-back and westward motion of the Loyalty arc continued. Continuing convergence resulted in a new subduction starting along the west coast of New Caledonia (Fig. 1) (Cluzel et al. 2001).

According to the available geochemical and isotopic data, the post-obduction granitoids may be related to a continental active margin setting and record the reactivation of subduction after the late Eocene obduction (Cluzel et al. 2005). Subduction-controlled convergence in the New Caledonia basin is marked by the inversion of Late Cretaceous graben and high-angle reverse faults that crosscut most of the Tertiary pile. The convergence is post-dated by the late Miocene (ca. 10 Ma) unconformity (Van de Beuque 1999). According to geologic evidence on land, the ophiolitic nappe was thrust over parautochthonous calcareous sedimentary rocks that contain a late Priabonian (33.7-35 Ma) micro fauna (Cluzel et al. 1998) and is unconformably covered by Miocene conglomerate. Therefore, the timing of granitoid intrusion is poorly constrained by stratigraphic evidence after ca. 34 Ma and before ca. 10 Ma. Previous age-dating of St Louis granodiorite, based on biotite and amphibole K-Ar data, provided Miocene apparent ages (Guillon 1975; Black et al. 1994). However, evidence for post magmatic tectonic and hydrothermal events is widespread and K-Ar data is questionable.

A better constraint on intrusion timing will allow the working hypothesis of an active margin setting for the granitoids to be tested.

Petrography and geochemistry of the granitoids.

The major occurrences of Tertiary granitoids are the Saint-Louis massif which is located on the West coast, 12 km to the East of Noumea, and the Koum-Borindi massif on the Eastern coast, 55 km to the North of Noumea (Fig. 2). Both are composed of one main pluton 2 to 4 km wide and of several stocks and sub-volcanic dykes. The granitoids intrude the Ophiolitic Nappe and its autochtonous basement that typically displays contact metamorphism. The granodiorites have neither ductile fabrics nor mineral preferred orientation and are likely to have been intruded in a static environment.

The St Louis massif is composed of relatively homogenous hornblende-biotite granodiorite containing numerous hypovolcanic dykes and comagmatic enclaves. It is typically composed of plagioclase, K-feldspar, quartz, biotite and hornblende. Zoned plagioclase may represent 40 to 50% of the whole rock and appears as an early phase, together with Fe-rich biotite commonly found as euhedral prismatic crystals, rarely as amphibole pseudomorphs. The amphibole is a poikilitic magnesian hornblende that contains pyroxene relicts. K-feldspar and quartz are late magmatic phases. Accessory minerals: apatite, zircon, rutile, magnetite and ilmenite are generally precocious; in contrast, epidote, muscovite and chlorite are related to post-magmatic alteration. Sinuous steeply dipping metre-thick microgranodiorite dykes have irregular boundaries, indicating intrusion in a still hot environment. In these rocks, euhedral amphibole crystals commonly contain biotite inclusions and numerous pyroxene relicts. Mesocratic hornblende-rich finer-grained enclaves, centimetre to decimetre or so in size, are locally abundant. They show similar mineral compositions and likely represent dismembered early co-magmatic dykes. St Louis intrusive rocks display homogeneous geochemical and

isotopic features consistent with magmas generated in an active margin setting, without evidence that little contamination by sediments or continental crust derived melts occurred (Cluzel et al. 2005).

The Koum/Borindi intrusive complex appears more heterogeneous and differentiated. Two main facies are present: a leucocratic tonalite, which is found in most dykes and intrusive stocks; and an amphibole-biotite bearing granodiorite that is apparently restricted to the main massif (Grand Koum). The tonalite facies exhibits prominent variations in quartz, plagioclase and K-feldspar contents. Plagioclase is always zoned and appears as an early phase together with biotite. The K-feldspar displays perthite and/or granophyre sub-solidus textures. In the granodiorite, the amphibole (magnesian hornblende) is generally scarce and frequently displays biotite pseudomorphs. Subvolcanic dykes with a similar mineralogy frequently display corroded and sometimes broken euhedral quartz grains; in these rocks amphibole is replaced by Mg-rich biotite pseudomorphs. Epidote, chlorite and muscovite are related to post-magmatic (hydrothermal?) alteration. Geochemical and isotopic features are almost similar to those of St Louis and infer a similar origin; however they have distinctly higher Nb and Ta contents irrespective of differentiation. In addition, some of the tonalite dykes display a strong depletion in HREE. These peculiar features have been interpreted as a consequence of the mineral heterogeneity of the sub-lithospheric mantle (Cluzel et al. 2005).

Granulite-facies xenolith.

Within the main granodiorite body of Koum, an unusual decimetre-scale xenolith has been found that bears a special importance on the understanding of the late Oligocene magmatic activity. The xenolith is a dark granular rock, lacking any preferred mineral orientation, plagioclase, garnet, biotite, and hercynite form a first stage granulite-facies paragenesis, while

margarite, epidote, "sericite", chlorite, and calcite appear as secondary phases. Opaque minerals and zircon are widespread.

Plagioclase is the major mineral phase and is formed of 1-3 mm grains of almost pure anorthite (An 99%) free of inclusions and zoning. Biotite is formed of 2-4 mm globular, often gently kinked crystals (biotite I) and smaller decussate flakes, 50-400 µm large on average (biotite II), interspersed within plagioclase grains. The larger biotite crystals (biotite I) were initially formed of Ti-rich siderophyllite and were changed into siderophyllite pseudomorphs. They contain abundant small granular opaque minerals (Fe and Fe-Ti oxides) forming concentric aureoles and ilmenite exsolution needles. Biotite I displays inclusion-free outer rims that obviously crystallised later. The outer rims of the large biotite crystals and the smaller flakes (biotite II) are typically free of opaque inclusions and, owing to their lower Fe-Ti contents, are likely to have crystallised at a lower temperature. Garnet occurs as poïkiloblastic almandine grains containing a few plagioclase, biotite and opaque mineral inclusions. Anorthite, garnet and biotite display no reactional boundary and therefore appear to be paragenetic.

Hercynite (Fe-Al spinel) appears as shapeless aggregates 2 to 4 mm in size, formed of 50-250 µm subhedral dark green grains. The boundary of hercynite aggregates with plagioclase is a microgranular destabilisation aureole made of corroded plagioclase grains, margarite, epidote, K-mica ("sericite") chlorite and minor calcite. These latter appear as secondary lower grade phases within reaction aureoles 20-40 µm thick, around hercynite aggregates.

Colourless acicular crystals of margarite (a calcic aluminosilicate of the mica group) are organised in sheaf-like aggregates. At the boundary between margarite and plagioclase grains, pure anorthite is locally changed into a less calcic anorthite (ca. An90) together with crystallisation of tiny calcite intergranular blobs. Hercynite and anorthite appear to have reacted together during a lower grade event, giving margarite, epidote, chlorite and "sericite"

while garnet and to a lesser extent biotite, were metastable. We used a multi-equilibrium thermo-barometric approach (Berman 1991) using the solid solution models of Berman (1988) for garnet and McMullin et al. (1991) for biotite. The primary paragenesis of the xenolith provides granulite-facies peak P-T conditions well constrained at ca. 9 Kbar and 700°C, consistent with the lower crust/uppermost mantle conditions (Cluzel et al. 2001). The secondary paragenesis (margarite, epidote, K-mica) infer re-equilibration at ca. 7 kbar and 580°C probably after or during the final consolidation of the host rock.

The Nd isotopic composition ($\varepsilon Nd_{25\ Ma}$ = + 5.1) is compatible with a lithospheric mantle origin and is closely similar to those of the granitoids (Table 1). A slightly higher radiogenic Sr content compared with the host granitoid (Cluzel et al. 2005) may be due to thermal reequilibration in the presence of crustal aqueous fluids. The REE contents (Table 1) are about four times higher than those of the host rock and the REE pattern of the "granulite" is parallel to that of granitoids, without any significant Eu anomaly (Fig 3). In an expanded REE pattern, the high Th-U concentrations are consistent with the other elements, while a large Ba-Sr (and Ca) positive anomaly occurs (Fig 4). The moderate FeO and TiO_2 concentrations (Table 1), the lack of any positive Eu anomaly in spite of very high Ca and Sr contents, and a relatively high K content rule out a cumulate origin. Considering the very high content in incompatible elements, it may be postulated that the xenolith has a magmatic origin and its geochemical and mineralogical features infer that it crystallised at lower crustal depth from an early batch of already evolved magma and was dragged upwards by the ascending granitoid magma. Consequently, even if the processes that produced this rock remains uncertain at that stage, it provides interesting constraints on the original depth of Oligocene granitoids.

U-Pb zircon geochronology.

Analytical methods

Zircons crystals were concentrated in the Magmas & Volcans Clermont-Ferrand Laboratory in using conventional separation techniques. After crushing, milling and sieving, the rock powder was passed over a Wilfley table. Zircon was further enriched using heavy liquids and finally magnetic separator. The final purification was done by handpicking under a binocular microscope.

U-Pb analyses were performed on the least magnetic (2° forward and side tilt at 2.2 A, using a Frantz magnetic barrier separator), mechanically abraded (Krogh 1982), and crack-free zircon grains. Zircon dissolution, chemical separation of U and Pb, and isotope analyses were carried out according to methods described by Paquette and Pin (2001). To avoid any contamination by material involved in U-Pb dating of Palaeozoic or older zircons, only new PFA Teflon® "Ludwig-type" dissolution capsules and beakers were used during this program. The U and Pb isotopes were measured on a VG Sector 54W mass spectrometer in multi-collector static mode. The isotopic ratios are corrected for mass discrimination (0.1 ± 0.015% per amu for Pb and U), isotopic tracer contribution and analytical blanks: 7 ± 2.5 pg for Pb and less than 1 pg for U. Initial common Pb is corrected for each fraction using the Stacey and Kramers (1975) two-step model. Data errors (2σ) of the zircon fractions and ages were calculated using the PBDAT 1.24 and Isoplot/Ex 2.49b programs (Ludwig 1993 and 2001).

Description of the zircons

The zircon grains from the three studied samples are very similar: euhedral, colourless, translucent with frequent apatite needles and rare opaque inclusions. Large crystals up to 300μm frequently occur with length/width ratios generally bracketed between 3 and 6, except

for the Koum granite where needle-shaped small zircons can be distinguished. Cathodoluminescence images (Fig. 5a) display a regular concentric oscillatory zoning, and in some rare occurrences, possible small inherited cores can be distinguished in SL9 and KO1 samples (Fig. 5b).

ID-TIMS results

Seven abraded and multi-grain zircon fractions from the Saint-Louis granodiorite SL9 sample were analysed. The results are shown in Table 2. Plotted on a Concordia diagram, five points are concordant and precisely define a U-Pb age at 27.4 ± 0.2 Ma (Fig. 6a). Fixing a lower intercept at this latter age, the two last points indicate a rough alignment with an upper intercept around 1.7 ± 0.1 Ga (Fig. 6b). The 27.4 Ma is interpreted as the intrusion time of the Saint-Louis granodiorite in the Late Oligocene. The poorly defined Palaeoproterozoic upper intercept may reflect the incorporation of older zircon grains, derived from a continental crust component (basement ?), during magma formation and/or ascent. This is confirmed by the occurrence of tiny cores within some zircon crystals.

Five abraded and multi-grain zircon fractions from the Koum granite KO1 sample were analysed. U contents are approximately twice those of the previous sample (Table 2). On the Concordia diagram, four points are concordant defining an age of 24.4 ± 0.1 Ma (Fig. 6c). The fifth fraction plots along a chord indicating an upper intercept at 348 +66/-70 Ma (Fig. 6d). The 24.4 Ma age is interpreted as the crystallisation of the zircons of KO1 sample. As for the previous sample, the Carboniferous upper intercept points to inheritance. In both samples, the intercept ages may only represent the mixing of different inherited zircon populations and consequently can provide geologically meaningless ages.

Four abraded and multi-grain zircon fractions from the BOR5 Borindi granulite-facies xenolith were analysed. U and Pb contents are similar to that of Saint Louis massif (Table 2).

The four fractions are concordant and define an age of 24.7 ± 0.2 Ma (Fig. 6e). In this sample, no older component was apparent. Considering the euhedral shape of the grains, the 24.7 Ma can be interpreted as the initial crystallisation of the zircons under granulite facies conditions.

Discussion.

The U-Pb dating of the Tertiary granitoids of New Caledonia provides evidence for a diachronous intrusion: Saint-Louis at 27.4 Ma and Koum-Borindi at 24.4 Ma. Considering an average subduction rate of 5 cm/year, the 7 Ma elapsed between obduction (stratigraphically constrained as post- 34.4 Ma) and the first magmatic episode allowed the subduction of ca. 350 km of oceanic crust, an amount consistent with the appearance of volcanic-arc magmas. The two massifs display roughly comparable isotopic features and are likely to have been generated from similar mantle sources. However, a relative enrichment in Nb and Ta of Koum-Borindi rocks compared to St Louis irrespective of a differentiation process, may be due to a contrasting amount of Nb and Ta receptors, i.e. mineral heterogeneity, in the mantle source (Cluzel et al., 2005). The 3 Ma time gap between the two episodes may represent the migration of a single subduction front with time. This interpretation is consistent with the location of the St Louis massif that is at present too close (ca. 50 km) to the paleo-trench as expressed by a -100 mGal gravity anomaly. The continuous westward migration of the trench-arc system related to the opening of the North Loyalty back-arc basin may have resulted in a relative eastward migration of the mantle wedge when the thinned continental or transitional crust of the Lord Howe rise/New Caledonia basin reached the trench (Fig 7). Alternatively, it may also represent a two stage evolution. The first one being related to a “normal” active margin that resulted from the birth of a new subduction along the west coast of New Caledonia a short time after obduction. The second step may be related to the older slab break-off triggered by the exhumation of the high-pressure metamorphic complex and the

isostatic uplift due to the partial subduction of the Norfolk ridge underneath the fore-arc lithosphere of the Loyalty arc (Fig 8a). This second step may have generated the more eastern Nb-rich Koum-Borindi magmas at 24 Ma by uplift and mixing of a limited amount of unmetasomatised peridotite to the mantle wedge (Cluzel et al., 2005).

The occurrence of tiny cores within some rare zircon crystals implies a small but real contribution of the continental crust or sedimentary material. However, this contamination did not significantly change the geochemical and isotopic signatures that remain close to those of intra-oceanic volcanic arcs. The lack of Mesozoic reworked zircon grains, together with the overall geochemical and isotopic features rules out the possibility for these granites to have been generated through the extensive melting of basement rocks (e.g. the pre-Cretaceous Central Chain greywackes). The occurrence of inherited zircons cores may be interpreted in terms of contribution of an old continental crust component to recent mantle-derived material, or alternatively of recycled zircons incorporated into the magma through the assimilation of clastic sediments. This may infer that zircons recording Palaeoproterozoic geological events are present in the lower part (possibly the lower crust) of the basement. However, the oldest rock ever found in New Caledonia is only 300 Ma old (Aitchison et al. 1998) and there is no known evidence for an older continental basement. However, the continental crust of the Grande Terre is ca. 30 km thick (Dubois et al. 1974) and our knowledge of the deep part of this crust is extremely limited. Alternatively, Palaeoproterozoic and Palaeozoic detrital zircons are known to exist in Late Cretaceous sandstone (Aronson and Tilton 1971; Aitchison et al. 1998) that form the autochthonous basement of the ophiolite, intruded by Oligocene granitoids. Although no Cretaceous sedimentary xenolith has been found yet, contamination by zircon-bearing sandstone is not unlikely.

We described above the first occurrence of a granulite-facies xenolith from New-Caledonia. This rock contains zircon grains characterised by the same U-Pb age (24.5 Ma) as

the enclosing granitoid. The euhedral zircon crystals are similar to those of the host-rock and record one single high-temperature event. Consequently, we interpret that result as dating zircon crystallization during the rock formation under granulite-facies conditions. As the granulite-facies xenolith is in isotopic equilibrium (Sr-Nd-Pb) with the host rock, we infer that the magma that transported it to the surface was generated in a mantle region were granulite-facies conditions prevailed, i.e. at a ca 30-35 km depth.

Regional correlation and inferences on Southwest Pacific evolution.

It is generally considered that convergence stopped in New Caledonia after obduction, e.g. at the Eocene-Oligocene boundary. In contrast, many workers attempted to establish correlations between the ophiolite of New Caledonia and the Northland – East Cape mafic allochthons of northern New Zealand that were obducted in the late Oligocene (Brothers and Delanoye 1982). This resulted in a model of diachronous obduction, which was further complicated by the supposed southward dip of the Northland subduction (Spörli 1989). More recently, it has been suggested that the ridge system that extends from the D'Entrecasteaux ridge to the Northland and including New Caledonia and the Three Kings ridge formed one single subduction/obduction system with a global "Australian" vergency (Aitchison et al. 1995, Meffre 1995; Cluzel et al. 2001; Bernardel et al. 2002). The subduction and roll-back of the Australian plate generated an Eocene-Oligocene volcanic arc propagating southwards, while the North Loyalty and proto-South Fiji back-arc basins opened (Fig. 7). Obduction occurred when the subduction zone reached continental margins, in the latest Eocene or earliest Oligocene in New Caledonia and late Oligocene in northern New Zealand (Fig. 7 and 8). Considering the new time constraints presented here, and the occurrence of ophiolite remnants dredged on the western Three Kings ridge (Bernardel et al. 2002) that forms the

missing link, it appears that convergence was actually still active in the northern part of the system (e.g. in New Caledonia) at least until the late Oligocene. It is worth noting that the reactivated subduction in New Caledonia was almost synchronous with Northland-East Cape obduction, giving the model more consistency. The post-obduction (Miocene) Northland arc was born when the Fiji-Tonga arc that propagated southwards reached the northern tip of North Island. It was followed by a rapid eastward slab roll-back and arc migration along the Veining-Meinesz transform zone, until it reached its present geometry.

Conclusion.

U-Pb zircon geochronology of the post-obduction granitoids provides new time constraints on the genesis of these active margin magmas. At ca. 27 Ma, a new subduction along the west coast of New Caledonia generated the active margin magmatism on the Grande Terre that replaced the extinct Loyalty arc. At ca. 24 Ma, the eastward shift of the magma activity and occurrence of relatively Nb-enriched magmas was either due to the older slab break-off; or alternatively, by the "collision" of the thinned eastern margin of the Lord Howe rise that provoked the eastward migration of the mantle wedge. The occurrence of a granulite-facies xenolith with identical U-Pb zircon age (24.5 Ma) and isotopic features (initial ε_{Nd} = 5.1) probably means that these slightly enriched magmas were generated within the lithospheric mantle beneath a continental crust of a normal thickness. Evidence for continuous convergence during the Oligocene tightly constrains the model of a continuous subduction/obduction system that extended over 3,000 km from the D'Entrecasteaux zone to the Northland Plateau in northern New Zealand.

Acknowledgements

Review by Dr. J.D. Kramers improved the overall clarity of the original version of the manuscript.

References.

Aitchison JC, Clarke GL, Cluzel D, Meffre S (1995) Eocene arc-continent collision in New Caledonia and implications for regional southwest Pacific tectonic evolution, Geology 23, pp 161-164

Aitchison JC, Ireland TR, Clarke GL, Cluzel D, Meffre S (1998) U/Pb SHRIMP age constraints on the tectonic evolution of New Caledonia and regional implications, Tectonophysics 299, pp 333-343

Aronson JL, Tilton GR (1971) Probable precambrian detrital zircons in New Caledonia and Southwest Pacific continental structure, Geol Soc Am Bull 82, pp 3449-3456

Auzende JM, Van de Beuque S, Régnier M, Lafoy Y, Symonds P (2000) Origin of New Caledonian ophiolites based on a French-Australian seismic transect. Marine Geol 162, pp 225-236

Berman RG (1988) Internally consistent thermodynamic data for minerals in the system Na_2O-K_2O-CaO-MgO-FeO-Fe_2O3-Al_2O3-TiO_2-H_2O-CO_2: representation, estimation, and high temperature extrapolation. Journal of Petrology 29, pp 445-522

Berman, RG (1991) Thermo barometry using multi-equilibrium calculations: a new technique, with petrological applications. Can Mineral 29, pp 833-855

Bernardel G, Carson L, Meffre S, Symonds P, Mauffret A (2002) Geological and morphological framework of the Norfolk Ridge to Three Kings Ridge region. Geoscience Australia Record, 2002/08

Black PM, Itaya T, Ohra T, Smith IE, Takagi M (1994) Mid-Tertiary magmatic events in New Caledonia: K-Ar dating of boninitic volcanism and granitoid intrusives, Geosci Repts of Shizuoka Univ 20, pp 49-53

Brothers RN Delanoye M (1982) Obducted ophiolites of North Island, New Zealand: origin, age, emplacement and tectonic implications for Tertiary and Quaternary volcanicity. N Z Journal of Geology and Geophysics 25, pp 257-274

Cluzel D, Chiron D, Courme MD (1998) Discordance de l'Eocène supérieur et événements pré-obduction en Nouvelle-Calédonie (Pacifique sud-ouest) C R Acad Sci Paris 327, pp 485-491

Cluzel D, Aitchison JC, Picard C (2001) Tectonic accretion and underplating of mafic terranes in the Late Eocene intra-oceanic fore-arc of New Caledonia (Southwest Pacific). Geodynamic implications. Tectonophysics 340, pp 23-60

Cluzel D, and Meffre S (2002) The Boghen Terrane (New Caledonia, SW Pacific): a Jurassic accretionary complex. Preliminary U-Pb radiochronological data on detrital zircon. C R Geoscience 334, pp 867-874

Cluzel D, Bosch D, Paquette JL, Lemennicier Y, Montjoie P, Ménot RP (2005) Late Oligocene granitoids of New Caledonia: a case for reactivated subduction and slab break-off. The Island Arc 14, pp 254-271

Dubois J, Launay J, Récy J (1974) Uplift movements in New Caledonia-Loyalty islands area and their plate tectonics interpretation, Tectonophysics 24, 133-150

Evensen, N.M., Hamilton, P.J. and O'Nions, R. K., 1978. Rare earth abundance in chondritic meteorites. Geochim. Cosmochim. Acta, 42, p. 1199-212.

Guillon JH (1975) Les massifs peridotitiques de Nouvelle-Calédonie. Type d'appareil ultrabasique stratiforme de chaîne récente, Mém ORSTOM Fr 76, 11-120

Krogh TE (1982) Improved accuracy of U-Pb zircon ages by the creation of more concordant systems using an air abrasion technique. Geoch Cosmochim Acta 46/4, pp 637-649

Ludwig KR (1993) Pbdat: a computer program for processing Pb-U-Th isotope data, version 1.24. United State Geological Survey, open-file report 88-542.

Ludwig KR (2001) User manual for Isoplot/Ex rev. 2.49. A geochronological toolkit for Microsoft Excel. Berkeley Geochronology Center Special Publication n°1a, 56 p.

Meffre S (1995) The developpement of arc-related ophiolites and sedimentary sequences in New Caledonia. PhD Thesis Univ. of Sydney, 236 p

McDonough W.F., Sun S., Ringwood A.E., Jagoutz E., Hofmann A.W. (1991). K, Rb and Cs in the earth and moon and the evolution of the earth's mantle. Geochim. Cosmochim. Acta, Ross Taylor symposium vol.

McMullin DW., Berman RG, Greenwood HJ (1991) Calibration of the SGAM thermobarometer for pelitic rocks using data from phase-equilibrium experiments and natural assemblages. Can Mineral 29, pp 889-908

Paquette JL and Pin C (2001) A new miniaturized extraction chromatography method for precise U-Pb zircon geochronology. Chem Geol 176/1-4, pp 313-321

Rawling TJ and Lister GS (2002) Large-scale structure of the eclogite-blueschist belt of New Caledonia. J of Struct Geol 24, pp 1239-1258

Régnier M (1988) Lateral variation of upper mantle structure beneath New Caledonia determined from P-wave receiver fonction: evidence for a fossil subduction zone. Geophys Jour 95, pp 561-577

Rigolot P and Pelletier B (1988) Tectonique compressive récente le long de la marge ouest de la Nouvelle-Calédonie : résultats de la campagne ZOE 400 du N/O Vauban (mars 1987). C R Acad Sci Paris 307, pp 179-184

Rodgers KA (1973) Felsic plutonic rocks from the southern portion of the New Caledonian ultramafic belt. Geol Mag GB 110, pp 431-446

Rodgers KA (1976) Ultramafic and related rocks from Southern New Caledonia. Bull BRGM Fr sect 4, 1, 33-55

Spörli KB (1989) Tectonic framework of Northland, New Zealand. The Royal Society of New Zealand Bull 26, 3-14

Stacey JS Kramers JD (1975) Approximation of terrestrial lead isotope evolution by a two-stage model. Earth Planet Sc Lett 26, pp 207-221

Van de Beuque S (1999) Evolution géologique du domaine péri-calédonien (sud-ouest Pacifique), Unpubl. PhD thesis Université de Bretagne Occidentale, 270 p

Figure captions.

Figure 1: synthetic sketch map of the Southwest Pacific region.

Figure 2: simplified geologic map of southern New Caledonia to show the relationship between the Oligocene granitoids and the ultramafic allochthon (CFZ = Cook Fracture Zone, VMFZ = Veining-Meinesz Fracture Zone)

Figure 3: Chondrite-normalised Rare Earth Elements patterns of the BOR5 granulite-facies xenolith compared with those of the Koum-Borindi intrusive complex (grey outline, after Cluzel et al, 2005) to show the high REE content inconsistent with a cumulative genesis. Normalising values are from Evensen et al,. (1978).

Figure 4: REE and trace elements expanded spiderdiagrams normalised to the primitive mantle (McDonnough et al,, 1991) to show high HFSE contents compared to the host granitoids (grey outline) and the prominent positive anomalies in Ba and Sr correlative of the very high Ca content of the rock (not represented). A slight depletion in K_2O may be due to "hydrothermal" alteration during low grade recrystallisation.

Figure 5: Scanning electron microscope cathodoluminescence images of zircon grains from Saint-Louis granite. (A) Euhedral grain with magmatic oscillatory zoning, (B) Euhedral grain crystallised around a small inherited core.

Figure 6: $^{206}Pb/^{238}U$ vs. $^{207}Pb/^{235}U$ concordia diagrams of conventional multi-grain analysis of zircons from New Caledonia samples.

Figure 7: speculative model for the Oligocene geodynamic setting of the SW Pacific (with location of the cross sections Fig 8a and 8b.

Figure 8: two-dimention models for the Late Oligocene geodynamic setting of New Caledonia and North Island of New Zealand (for location, see Fig 5).

Table contents.

Table 1: Whole-rock major and trace element contents with additional Nd isotopic composition for BOR5 granulite sample.

Table 2: ID-TIMS U-Pb zircon analysis data for studied samples from New Caledonia.

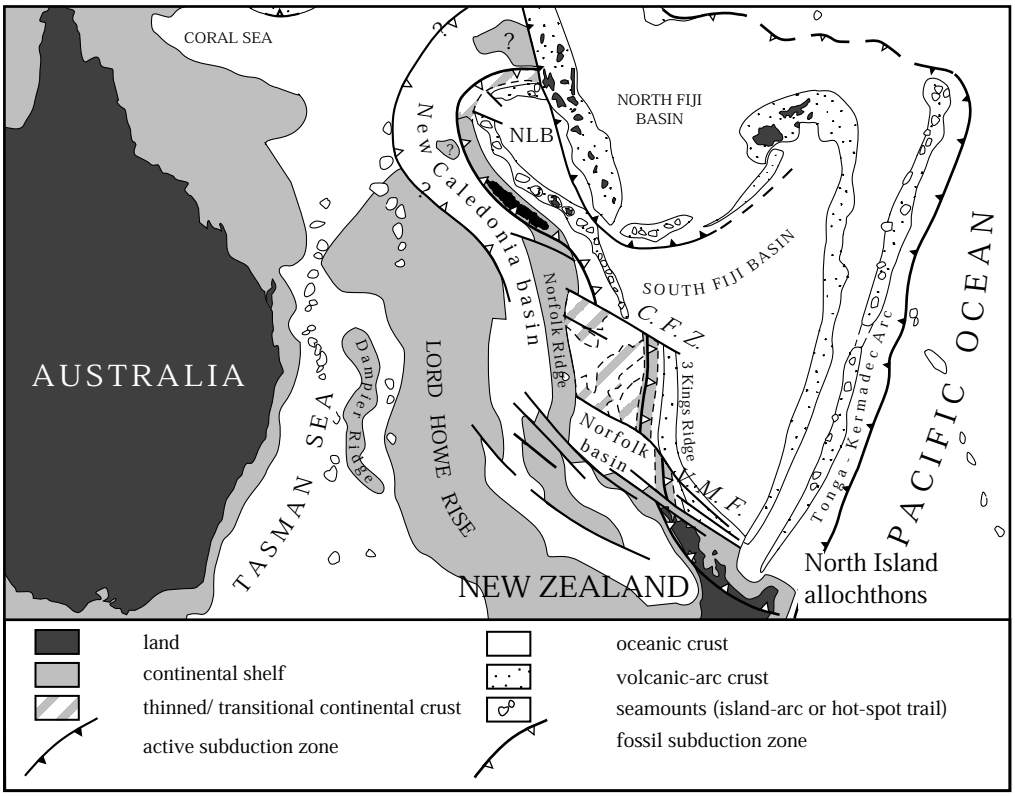

Paquette and Cluzel, 2006 Figure 1

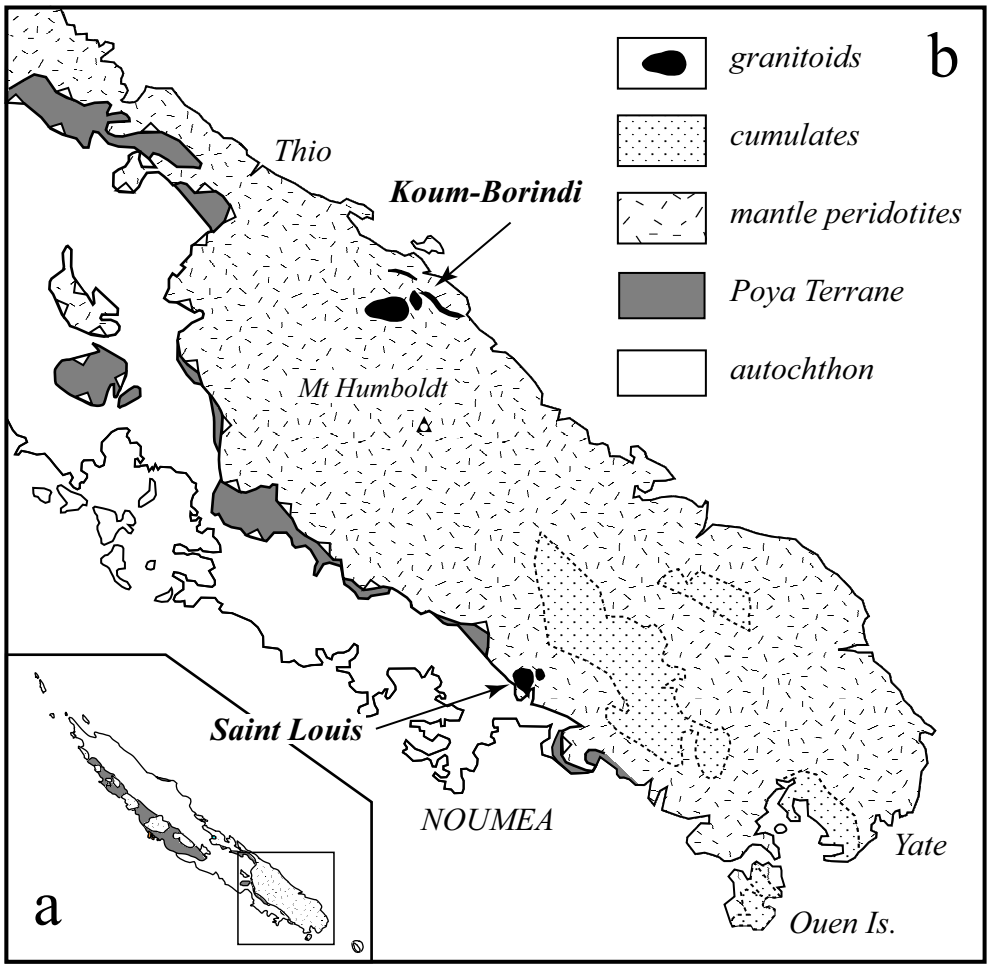

Paquette and Cluzel, 2006 Figure 2

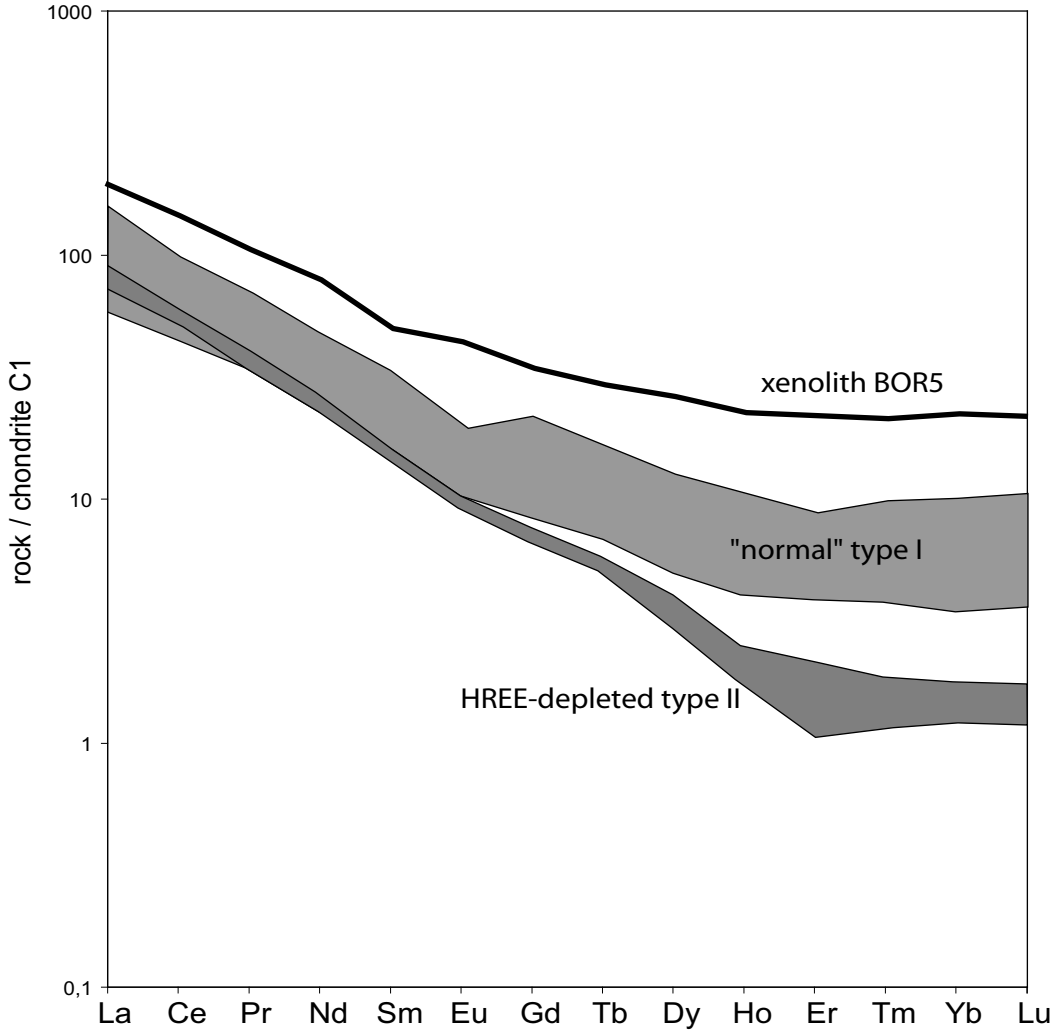

Paquette and Cluzel, 2006 Figure 3

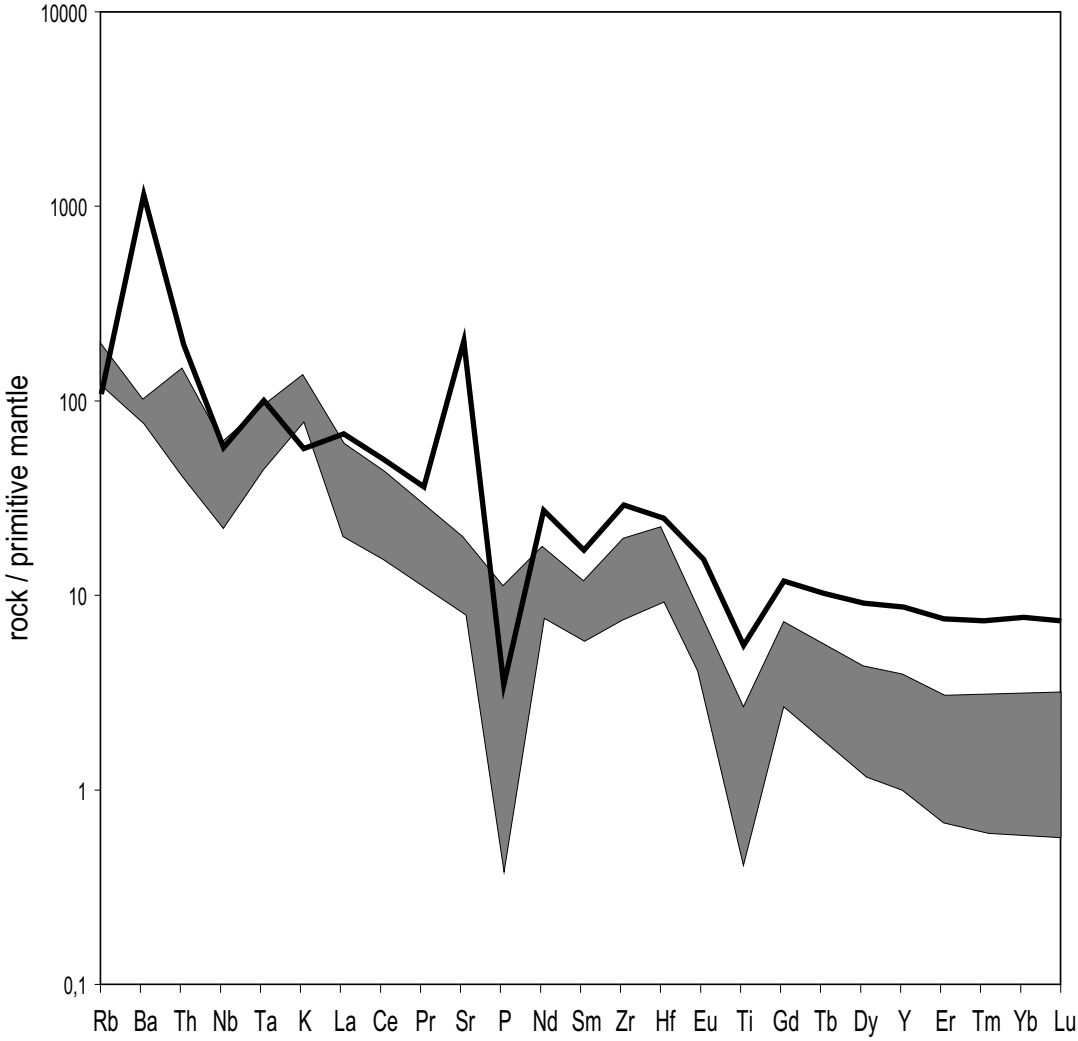

Paquette and Cluzel, 2006 Figure 4

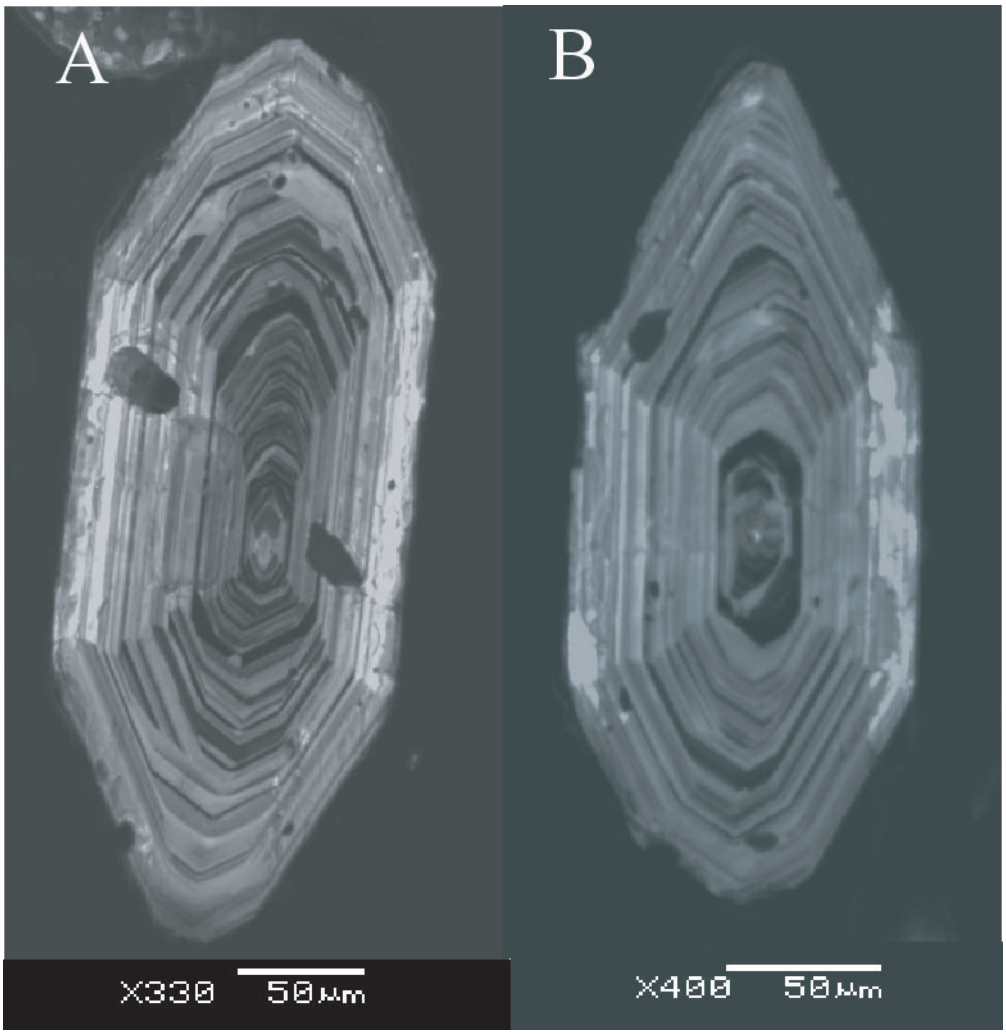

Paquette and Cluzel, 2006 Figure 5

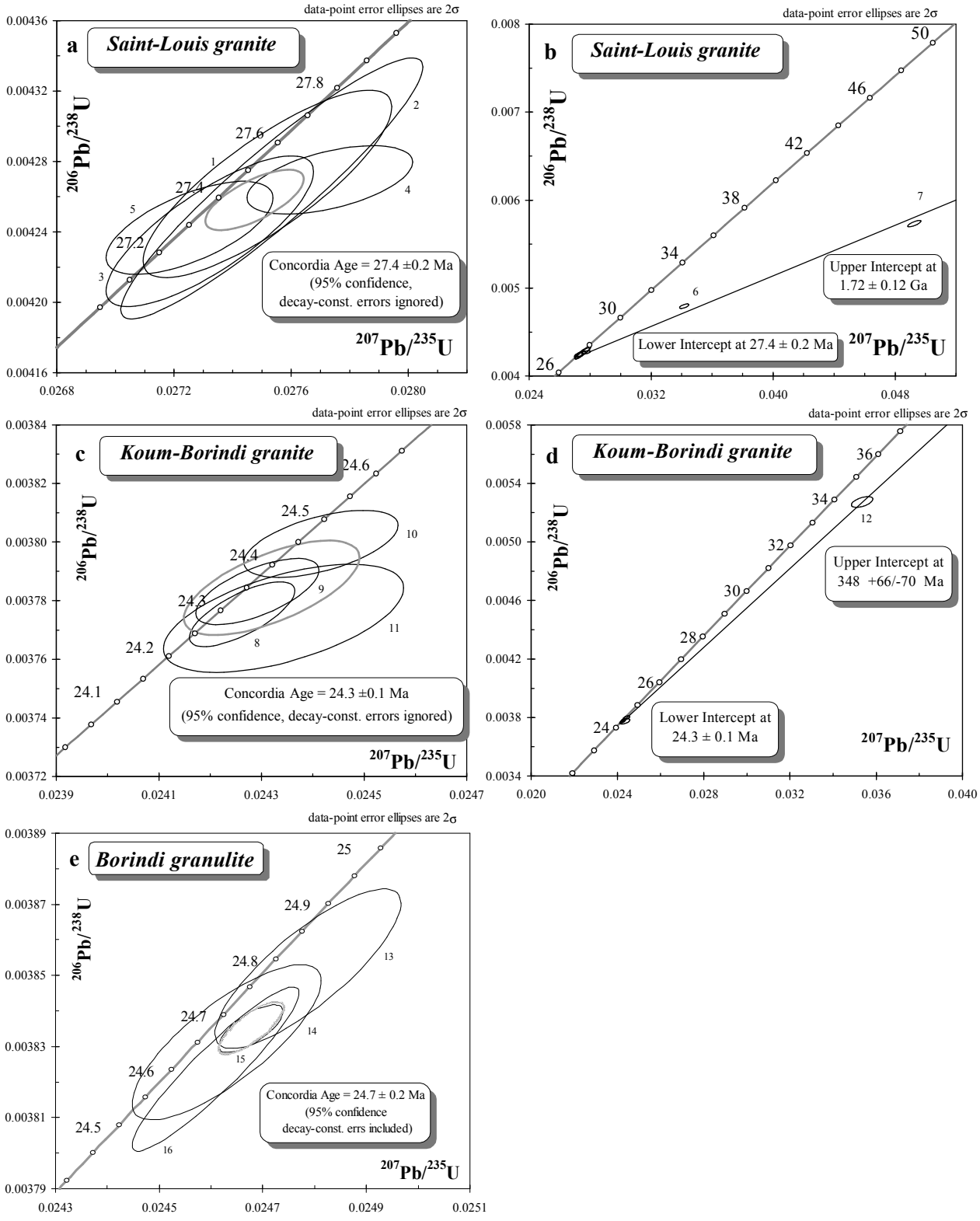

Paquette & Cluzel 2006 Figure 6

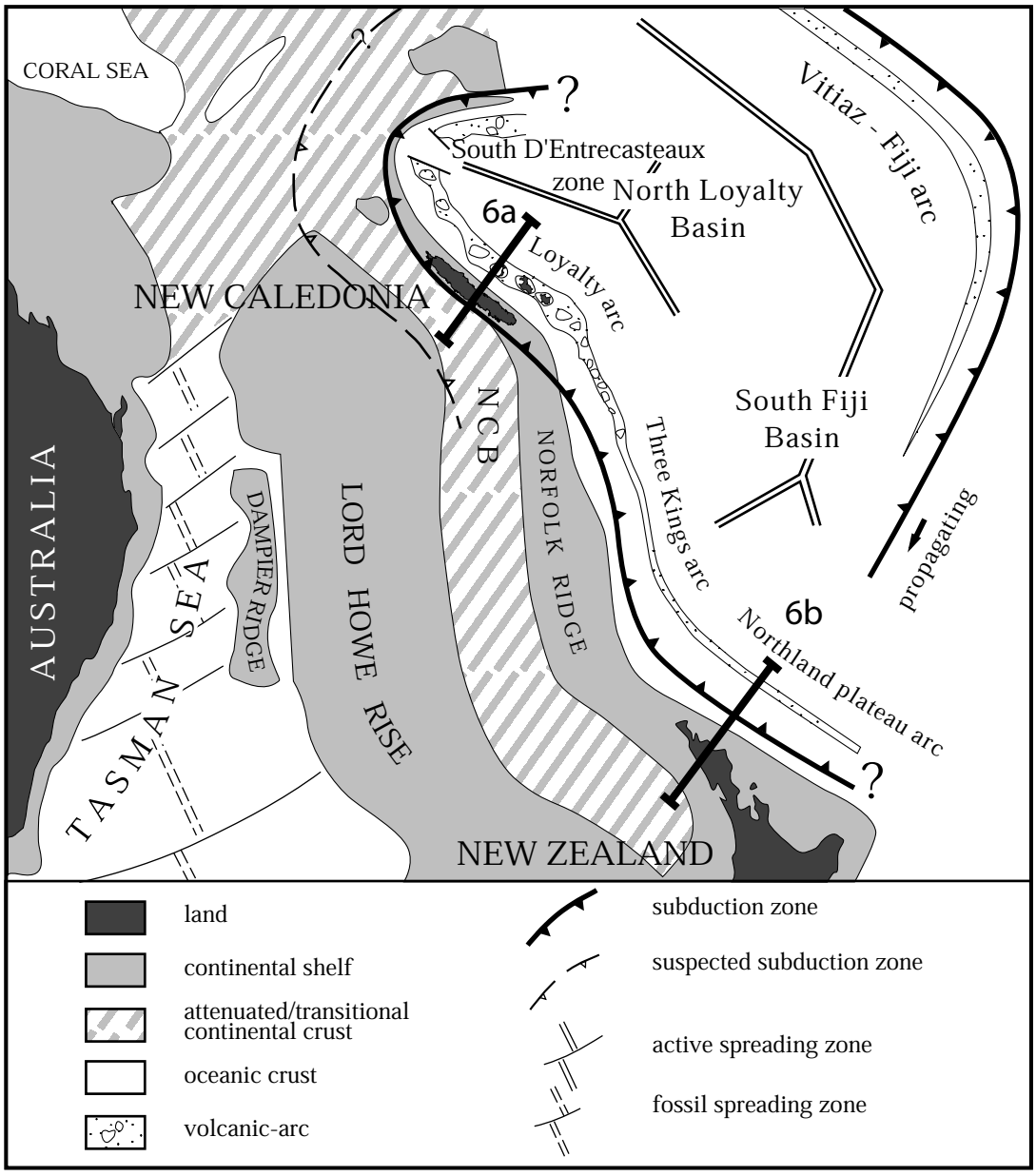

Paquette and Cluzel, 2006 Figure 7

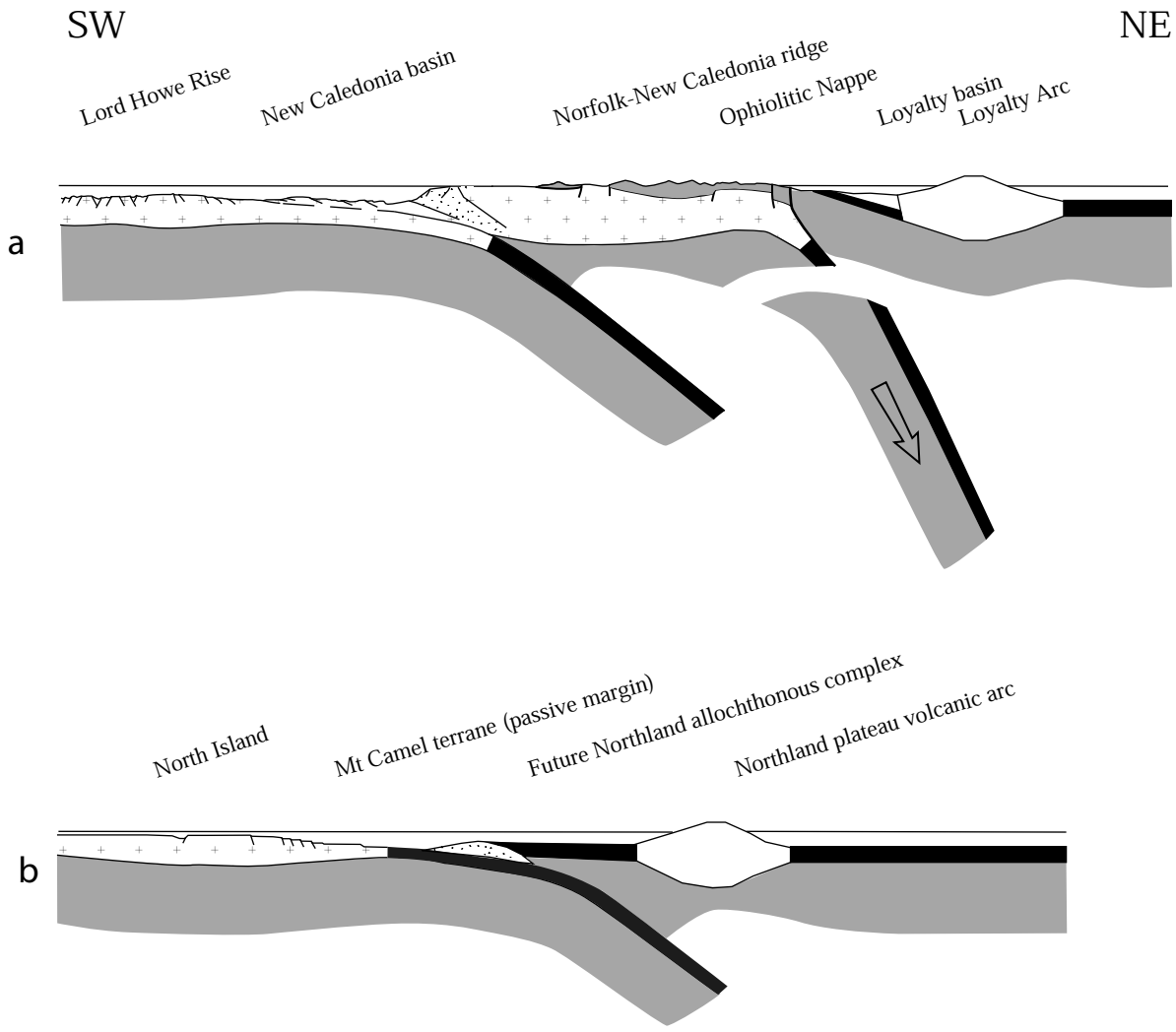

Paquette and Cluzel, 2006 Figure 8

Sample	weight %	Sample	µg/g	Sample	µg/g
SiO_2	35.51	Cs	4.5	Th	16.5
Al_2O_3	33.26	Rb	71	U	5.7
Fe_2O_3	11.71	Sr	4277		
MnO	0.07	Ba	8028	La	46.5
MgO	2.65	V	72	Ce	88.8
CaO	12.61	Mo	4.4	Pr	10.0
Na_2O	0.30	Cr	140	Nd	37.1
K_2O	1.70	Co	24	Sm	7.6
TiO_2	1.20	Ni	80	Eu	2.6
P_2O_5	0.05	Zn	257	Gd	7.1
H2O+	0.98	Ga	33	Tb	1.1
Total	100.04	Y	40	Dy	6.7
		Zr	326	Ho	1.3
		Nb	41	Er	3.6
		Hf	7.7	Yb	3.8
		Ta	4.1	Lu	0.6

$^{87}Sr/^{86}Sr$	$^{147}Sm/^{144}Nd$	$^{143}Nd/^{144}Nd$	$\varepsilon_{(25Ma)}$
0.70438 ± 1	0.1087	0.512884 ± 7	+5.1

Paquette & Cluzel 2006 Table 1

Sample n°	Weight mg	U	Pb rad	206Pb 204Pb	208Pb 206Pb	206Pb 238U	207Pb 235U	207Pb 206Pb	206Pb 238U	207Pb 235U	207Pb 206Pb
		conc. (ppm)			*atomic*	*ratios*			*apparent ages (Ma)*		
	Saint-Louis granite										
1	0.232	608	2.60	721	0.1670	0.004267 ± 1.0	0.02752 ± 1.3	0.04677 ± 0.7	27.5	27.6	37.6
2	0.208	993	4.19	709	0.1548	0.004265 ± 1.4	0.02753 ± 1.5	0.04683 ± 0.5	27.4	27.6	40.4
3	0.155	564	2.40	1051	0.1551	0.004240 ± 0.8	0.02732 ± 1.1	0.04673 ± 0.6	27.3	27.4	35.5
4	0.166	619	2.65	570	0.1796	0.004269 ± 04	0.02773 ± 0.8	0.04711 ± 0.7	27.5	27.8	54.7
5	0.139	635	2.69	910	0.1527	0.004242 ± 0.5	0.02725 ± 0.9	0.04659 ± 0.7	27.3	27.3	28.3
6	0.172	633	3.04	660	0.1676	0.004794 ± 0.4	0.03417 ± 0.7	0.05169 ± 0.5	30.8	34.1	272
7	0.169	418	2.43	1072	0.1508	0.005733 ± 0.5	0.04927 ± 0.7	0.06233 ± 0.4	36.9	48.8	685
	Koum-Borindi granite										
8	0.300	1004	3.76	1870	0.1250	0.003775 ± 0.2	0.02426 ± 0.3	0.04664 ± 0.2	24.3	24.3	29.2
9	0.169	1477	5.99	1315	0.2252	0.003783 ± 0.2	0.02429 ± 0.4	0.04657 ± 0.3	24.3	24.4	27.3
10	0.130	1172	4.38	1283	0.1255	0.003799 ± 0.2	0.02442 ± 0.5	0.04661 ± 0.4	24.4	24.5	29.2
11	0.143	978	3.64	1055	0.1336	0.003774 ± 0.4	0.02434 ± 0.8	0.04678 ± 0.7	24.3	24.4	38.1
12	0.123	952	5.00	1627	0.1313	0.005274 ± 0.6	0.03535 ± 1.2	0.04862 ± 1.0	33.9	35.3	129
	Borindi granulite										
13	0.237	733	2.78	1599	0.0839	0.003852 ± 0.5	0.02479 ± 0.6	0.04667 ± 0.3	24.8	24.9	32.4
14	0.274	996	3.71	2994	0.0755	0.003835 ± 0.1	0.02468 ± 0.2	0.04667 ± 0.1	24.7	24.8	32.4
15	0.235	685	2.57	1609	0.0784	0.003831 ± 0.5	0.02463 ± 0.6	0.04663 ± 0.4	24.7	24.7	30.2
16	0.345	871	3.26	1813	0.0758	0.003824 ± 0.5	0.02461 ± 0.5	0.04668 ± 0.2	24.6	24.7	32.8

Individual analyses were performed on the least magnetic (2° forward and side tilt at 2.2 A using a Frantz Isodynamic magnetic barrier separator) crack-free zircon grains. The isotopic ratios are corrected for mass discrimination (0.1 ± 0.015 % per amu for Pb and U), isotopic tracer contribution and analytical blanks: 7 ± 3 pg for Pb and less than 1 pg for U. Initial common Pb is determined for each fraction in using the Stacey & Kramers (1975) two-step model. Relative errors are quoted at the 2σ level.

Paquette & Cluzel, 2006 Table 2